

Structural phase transition in the ordered fluorides $M^{II}ZrF_6$ ($M^{II}=Co,Zn$). II. Brillouin and Raman scattering study

This article has been downloaded from IOPscience. Please scroll down to see the full text article.

1990 J. Phys.: Condens. Matter 2 7387

(<http://iopscience.iop.org/0953-8984/2/36/002>)

View [the table of contents for this issue](#), or go to the [journal homepage](#) for more

Download details:

IP Address: 171.66.16.103

The article was downloaded on 11/05/2010 at 06:05

Please note that [terms and conditions apply](#).

Structural phase transition in the ordered fluorides $M^{II}ZrF_6$ ($M^{II} = Co, Zn$): II. Brillouin and Raman scattering study

V Rodriguez†, M Couzi†, A Tressaud‡, J Grannec‡, J P Chaminade‡ and C Ecolivet§

† Laboratoire de Spectroscopie Moléculaire et Cristalline (URA 124 CNRS), Université de Bordeaux I, 33405 Talence Cédex, France

‡ Laboratoire de Chimie du Solide du CNRS (CNRS), Université de Bordeaux I, 33405 Talence Cédex, France

§ Groupe de Physique Cristalline (URA 40804 CNRS), Université de Rennes I, 35042 Rennes Cédex, France

Received 6 February 1990, in final form 8 May 1990

Abstract. The first-order ferroelastic $Fm\bar{3}m \leftrightarrow R\bar{3}$ structural phase transition occurring in ordered $M^{II}ZrF_6$ fluorides ($M^{II} = Co, Zr$) is studied by means of Brillouin and Raman scattering experiments. The Brillouin data obtained with a $CoZrF_6$ single crystal show that the elastic constant C_{44} does not change in the cubic phase, when the transition temperature ($T_c = 272 \pm 1$ K) is approached from above. The Raman spectra of $CoZrF_6$ and $ZnZrF_6$ in the cubic phase are consistent with group-theoretical predictions; in the rhombohedral phase, the spectra exhibit a splitting of the ν_5 triply degenerate bending mode of the $M^{II}(Zr)F_6$ octahedra and show the existence of two soft rotatory modes of these octahedra. From these results and group-theoretical considerations, it is concluded that the phase transition can be considered as improper ferroelastic, driven by octahedra rotations; possibly, an intermediate behaviour between true displacive and order–disorder regimes takes place in these materials.

1. Introduction

In paper I of this series [1], the ferroelastic structural phase transition occurring in the mixed fluorides $CoZrF_6$ and $ZnZrF_6$ (ordered ReO_3 -type structure) has been investigated using neutron and x-ray diffraction techniques. This phase transition is of first order, and connects a high-temperature cubic phase ($Fm\bar{3}m$) to a low-temperature rhombohedral modification ($R\bar{3}$). The transition temperature is 272 ± 1 K for $CoZrF_6$ and 310 ± 1 K for $ZnZrF_6$ [1].

From a complete structural determination of $CoZrF_6$ at different temperatures, three order parameters for the phase transition have been measured, namely the spontaneous strain e_s , the rotation coordinate of the $Co(Zr)F_6$ octahedra around the threefold axis, R , and the internal deformation coordinate of these octahedra, Q [1]. Clearly, the values obtained for the Q coordinate always remain very small in the rhombohedral phase, showing that the octahedra are essentially rigid bodies. As a consequence, the contribution of this parameter to the transition mechanism is not expected to be very important. In contrast, due to the strong variations obtained for e_s and R , it can be

concluded that these parameters are much more relevant in the transition mechanism [1]. It is also important to point out that the coupling between e_s and R is linear in e_s and quadratic in R (see paper III [2]).

Thus, the diffraction techniques made it possible to measure the static properties of the order parameters, which represent the temperature evolution of the mean amplitude of atomic displacements through the phase transition. However, it is not possible from these experiments to draw any conclusion about the driving forces responsible for the transition. For such a purpose, the study of the dynamical properties of the order parameters, i.e. of the associated susceptibilities [3], must be carried out. As will be shown from group-theoretical considerations (see section 3), the susceptibilities of the R and Q order parameters are related to the frequencies of a rotatory mode and of an internal bending vibration of the octahedra, respectively. These modes are Raman-active in the cubic and/or the rhombohedral phase, but are always infrared-inactive. On the other hand, the susceptibility of the elastic strain e_s is related to the elastic constant C_{44} (shear mode), which can be measured by means of ultrasonic or Brillouin scattering experiments. Then, anomalies may be expected in the temperature evolution of these dynamical parameters, in the vicinity of the transition temperatures, depending on whether the octahedra rotation and/or the elastic strain are driving order parameters.

The present paper (II) of this series is devoted to an experimental study of the ferroelastic phase transition of the CoZrF_6 and ZnZrF_6 ordered fluorides by means of Raman and Brillouin scattering experiments, thus allowing an unambiguous description of the transition mechanism.

2. Experimental details

Sample preparation has been described in the preceding paper (I) of this series [1]. Red-purple coloured CoZrF_6 single crystals, in the shape of parallelepipeds up to $5 \times 5 \times 5 \text{ mm}^3$ size and with natural faces developed perpendicular to the crystallographic cubic axes, were used for Raman and Brillouin scattering experiments. Only powdered samples of ZnZrF_6 are available [1]. Furthermore, due to the rather strong first-order character of the transition [1], single crystals of CoZrF_6 (cubic phase) undergo important damage when passing through the transition temperature; as a result, polycrystalline samples will be used in rhombohedral CoZrF_6 .

The Raman spectra of CoZrF_6 and ZnZrF_6 have been recorded either on Coderg T 800 or Dilor Z 24 triple monochromator instruments equipped for detection with cooled RCA and Hamamatsu photomultipliers, respectively, both of them being coupled with photon counting systems. In the case of CoZrF_6 , the 674.4 nm emission line of a Spectra Physics krypton ion laser has been used for excitation, in order to avoid light absorption and to get rid of luminescence or fluorescence signals (coming from Co^{2+}) superimposed on Raman lines. For the colourless ZnZrF_6 samples, the 514.5 nm emission line of a Spectra Physics argon ion laser has been used. The spectral slit widths were about 2 to 4 cm^{-1} . Low-temperature measurements have been made down to $\sim 80 \text{ K}$ with a C4N cryostat from Dilor; some experiments down to $\sim 20 \text{ K}$ have also been made, using a Cryodine model 20 helium refrigerator, equipped with the sample holder modification described in [4]. For measurements up to $\sim 400 \text{ K}$, the heating system of a Coderg cryostat has been used. In all cases, temperature regulation was better than $\pm 0.5 \text{ K}$.

The Brillouin scattering set-up mainly consists of a five-pass piezoelectrically scanned Fabry Perot interferometer, which is controlled by a microcomputer. This set-up has

been described previously [5] and the only modifications made here were due to the use of a krypton ion laser (Coherent Radiation) at 647.1 nm. We used a free spectral range of 57 GHz.

CoZrF_6 crystals were morphologically oriented along a (100) direction and immersed in a cell containing silicone oil in order to prevent deterioration of the crystal faces by water at higher temperatures. This cell was placed inside a home-made oven, where temperature stability was about 0.5 K.

3. Group theory and lattice dynamics

From classical factor-group analysis [6] the enumeration of the zone-centre modes ($\mathbf{k} = 0$) of $\text{M}^{\text{II}}\text{ZrF}_6$ ordered fluorides in the cubic phase ($Fm\bar{3}m$) is determined as follows:

$$\Gamma_{\text{vib}} = A_{1g} + E_g + F_{1g} + F_{2g} + 4F_{1u} + F_{2u}.$$

This enumeration includes the $\mathbf{k} = 0$ acoustic modes (F_{1u}) with zero frequency. The Raman-active representations are $A_{1g}(\alpha_{xx} + \alpha_{yy} + \alpha_{zz})$, $E_g(\alpha_{xx} + \alpha_{yy} - 2\alpha_{zz}, \alpha_{xx} - \alpha_{yy})$ and $F_{2g}(\alpha_{xy}, \alpha_{xz}, \alpha_{yz})$ [7]. A_{1g} corresponds to the totally symmetric stretching mode of the $\text{M}^{\text{II}}(\text{Zr})\text{F}_6$ octahedra (ν_1), E_g to a degenerate stretching mode (ν_2) and F_{2g} to a triply degenerate bending mode (ν_5). The optically inactive F_{1g} representation corresponds to the triply degenerate rotatory mode of the octahedra (ν_R). One can note that ν_5 (F_{2g}) and ν_R (F_{1g}) are associated respectively with the order parameters Q and R previously determined [1]. In addition, the elastic strain e_s measured in the rhombohedral phase [1] is connected to the e_{xy} (e_6), e_{xz} (e_5) and e_{yz} (e_4) strain tensor components with F_{2g} symmetry (shear mode) in the cubic phase.

In the rhombohedral phase, with $R\bar{3}$ space group, one gets:

$$\Gamma_{\text{vib}} = 3A_g + 3E_g + 5A_u + 5E_u.$$

The $3A_g(\alpha_{xx} + \alpha_{yy}, \alpha_{zz})$ and the $3E_g(\alpha_{xx} - \alpha_{yy}, \alpha_{xy}; \alpha_{xz}, \alpha_{yz})$ modes are Raman-active.

Table 1 gives the compatibility relations between irreducible representations in $Fm\bar{3}m$ and $R\bar{3}$ space groups. Thus, the ν_5 mode (F_{2g}) is expected to be split into two Raman-active components ($F_{2g} \rightarrow A_g + E_g$) while the inactive rotatory mode ν_R (F_{1g}) gives rise to two Raman-active components ($F_{1g} \rightarrow A_g + E_g$) in the $R\bar{3}$ phase.

It should also be pointed out that the transition $Fm\bar{3}m \leftrightarrow R\bar{3}$ can be described by a two-step mechanism, involving a hypothetical intermediate phase with $R\bar{3}m$ space group (table 1) where octahedra rotations are not allowed. The order parameter for the $Fm\bar{3}m \leftrightarrow R\bar{3}m$ hypothetical transition has F_{2g} symmetry (ν_5 mode and acoustical shear mode). So, it would be a 'proper' ferroelastic transition necessarily of first order because the F_{2g} representation does not fulfil Landau criteria [8]. Nevertheless, the direct transition $Fm\bar{3}m \leftrightarrow R\bar{3}$ is possible, induced by the F_{1g} representation (table 1), which contains the rotatory mode ν_R ; in that case, F_{2g} also induces the unity representation of $R\bar{3}$, since this space group is also a subgroup of $R\bar{3}m$ (table 1). Thus, two different mechanisms can be expected for the $Fm\bar{3}m \leftrightarrow R\bar{3}$ phase transition:

(i) The F_{1g} rotatory mode ν_R represents the primary order parameter, and the F_{2g} strain is a secondary order parameter ('improper' ferroelastic transition); then, the transition could be either of second order or of first order, since the F_{1g} representation

Table 1. Compatibility relations of lattice vibrations in cubic and rhombohedral phases for the ordered $M^{II}ZrF_6$ mixed fluorides. The full and broken heavy lines indicate the symmetry of the order parameter for the $Fm\bar{3}m \leftrightarrow R\bar{3}$ and the $Fm\bar{3}m \leftrightarrow R\bar{3}m$ transitions, respectively).

$Fm\bar{3}m (O_h^5)$		$R\bar{3}m (D_{3d}^5)$		$R\bar{3} (S_6^2)$
Γ_1^+/A_{1g} (1)		Γ_1^+/A_{1g} (2)		Γ_1^+/A_g (3)
Γ_2^+/A_{2g}		Γ_2^+/A_2 (1)		$\Gamma_2^+, \Gamma_3^+/E_g$ (3)
Γ_3^+/E_g (1)		Γ_3^+/E_g (3)		
Γ_4^+/F_{1g} (1)				
Γ_5^+/F_{2g} (1)				
Γ_1^-/A_{1u}		Γ_1^-/A_{1u} (1)		Γ_1^-/A_u (5)
Γ_2^-/A_{2u}		Γ_2^-/A_{2u} (4)		$\Gamma_2^-, \Gamma_3^-/E_u$ (5)
Γ_3^-/E_u		Γ_3^-/E_u (5)		
Γ_4^-/F_{1u} (4)				
Γ_5^-/F_{2u} (1)				

fulfils Landau criteria [8] (remember that these criteria are only necessary conditions allowing second-order phase transitions).

(ii) The F_{2g} strain is still the primary order parameter as for the $Fm\bar{3}m \leftrightarrow R\bar{3}m$ transition, but it 'triggers' [9–11] the F_{1g} octahedra rotation via a non-linear coupling mechanism (see paper III [2]) in order to achieve the $R\bar{3}$ symmetry; in that case, the transition would be 'proper' ferroelastic, necessarily of first order.

Since the $Fm\bar{3}m \leftrightarrow R\bar{3}$ transition is observed of first order [1], either mechanism (i) or (ii) is possible. The study of the behaviour of the C_{44} elastic constant associated with the F_{2g} strain components allows one to determine whether mechanism (i) or (ii) is actually taking place in $M^{II}ZrF_6$ materials. Indeed, in case (i), C_{44} is expected to be essentially constant in both cubic and $R\bar{3}$ rhombohedral phases, with a step-like variation at the transition temperature T_c , whereas in case (ii), C_{44} should exhibit an important softening in both phases, when T_c is approached from both sides [12]. Thus, Brillouin scattering experiments close to T_c are decisive to solve this problem. On the other hand, owing to the thermal variations observed for the order parameter R [1] (displacive mechanism) a softening of the frequency of the rotatory mode ν_R is expected to occur

Table 2. Brillouin shifts observed with cubic CoZrF_6 single crystal at different temperatures, in backscattering geometry ($\lambda_0 = 647.1$ nm).

T (K)	Brillouin shift $\Delta\nu$ (GHz)	
	$\Delta\nu_{\text{T}}(\pm 0.2)$	$\Delta\nu_{\text{L}}(\pm 0.4)$
293	14.14	34.85
321	13.67	33.80
348	13.48	33.50

close to T_c , in both cases (i) and (ii); as mentioned above, the two components of ν_{R} in the $R\bar{3}$ phase are Raman-active.

4. Results and discussion

4.1. Brillouin scattering

Brillouin scattering spectra of single crystals of CoZrF_6 have been recorded in the cubic phase, at three different temperatures (348, 321 and 293 K) approaching $T_c = 272$ K from above, but due to the polycrystalline state of samples below T_c , measurements were not performed in the rhombohedral phase.

Experiments were performed in a backscattering geometry in order to study phonons propagating along the $[100]$ directions. In principle this geometry only allows the observation of longitudinal modes [13] but, probably due to a large collecting angle ($f/4$), longitudinal and transverse modes were simultaneously observed. These modes are related to the elastic constants C_{11} and C_{44} by the relations

$$\rho V_{\text{L}}^2 = C_{11} \quad \rho V_{\text{T}}^2 = C_{44} \quad (1)$$

where V_{L} , V_{T} and ρ are respectively the phase velocity of longitudinal and transverse modes and the mass density of the crystal.

The Brillouin shift $\Delta\nu$ measured in Brillouin scattering involves not only the sound velocity but also the refractive index n as indicated by the well known formula [14]:

$$\Delta\nu = (2nV/\lambda_0) \sin(\theta/2) \quad (2)$$

where λ_0 is the laser wavelength (6471 Å) and θ is the scattering angle (180°).

In such a case the evolution of $\Delta\nu$ versus T depends also on the variations of $n(T)$, but the refractive index is not expected to vary dramatically in the relatively small temperature interval (50 K) where measurements have been performed. Then in a first approximation, we can take the square of the Brillouin shifts as proportional to the elastic constants.

Table 2 summarises the results obtained with CoZrF_6 . These results show that C_{44} remains essentially constant when T_c is approached from above; indeed, the small increase of $\Delta\nu_{\text{T}}$ with decreasing temperature, as well as that noticed for $\Delta\nu_{\text{L}}$, must be related to anharmonic effects associated with thermal expansion of the crystal lattice. In other words, it can be concluded that the $Fm\bar{3}m \leftrightarrow R\bar{3}$ phase transition is 'improper' ferroelastic (see section 3).

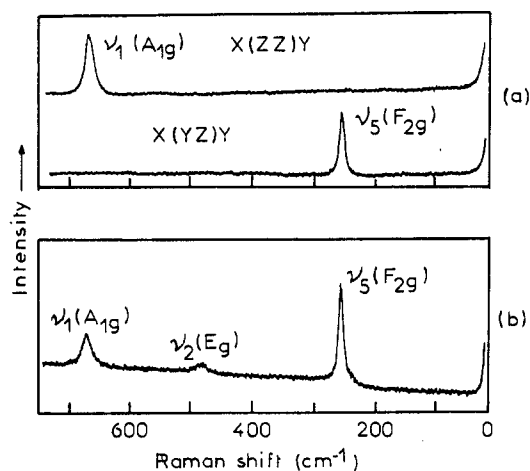


Figure 1. The Raman spectra of (a) CoZrF₆ single crystal (295 K) and (b) powdered ZnZrF₆ in the $Fm\bar{3}m$ cubic phase.

4.2. Raman scattering

Figure 1 shows the Raman spectra of single-crystal CoZrF₆ (295 K) and of powdered ZnZrF₆ (315 K) in the cubic phase $Fm\bar{3}m$. The assignment of these spectra is straightforward owing to the group-theoretical predictions (see section 3) and to the polarisation selections observed with CoZrF₆. So, the ν_1 mode (A_{1g}) is observed at 670 cm⁻¹ in both compounds and ν_5 (F_{2g}) at 249 and 253 cm⁻¹ in CoZrF₆ and ZnZrF₆, respectively. The ν_2 mode (E_g) appears as a broad line centred around 480 cm⁻¹ for ZnZrF₆, but this mode cannot be observed in the case of CoZrF₆, probably because its intensity is too weak.

In the rhombohedral phase (figure 2), one can notice the splitting of ν_5 , according to the scheme $F_{2g} \rightarrow A_g + E_g$ (table 1), and the appearance of two modes at low frequency, assigned to the two components of the rotatory mode, issued from the inactive ν_R mode ($F_{1g} \rightarrow A_g + E_g$). It is worth noting that the presence of two Raman-active components for ν_R confirms unambiguously the $R\bar{3}$ space group, since only one component would be Raman-active for $R\bar{3}m$ according to the scheme (table 1) F_{1g} (inactive) $\rightarrow A_{2g}$ (inactive) + E_g (Raman-active). The direct assignment of the ν_5 and ν_R components in terms of A_g and E_g symmetry is not possible on powdered samples. Nevertheless, if we refer to previous studies performed on CsSbF₆ single crystal in the $R\bar{3}$ rhombohedral phase [15, 16], the most intense component of ν_5 , which is also that of highest frequency (figure 2), has been attributed to E_g symmetry, and the second one to A_g symmetry. On the other hand, lattice dynamics calculations performed on rhombohedral AlF₃ ($R\bar{3}c$) indicate that the ν_R component of highest frequency has A_g symmetry whereas the second one has E_g symmetry [17]. Probably, the same holds true in CoZrF₆ and ZnZrF₆ as for the assignment of the ν_5 and ν_R components in the $R\bar{3}$ phase.

Figure 3 shows the temperature variations of the ν_5 and ν_R mode frequencies through the $Fm\bar{3}m \leftrightarrow R\bar{3}$ transition. Obviously, ν_5 behaves as a 'hard' mode, but the frequency splitting observed in the rhombohedral phase is temperature-dependent; this behaviour can be accounted for by an anharmonic coupling between the order parameter Q associated with the ν_5 mode and the elastic strain components of the same symmetry (see paper III [2]). In other words, the frequency splitting of the ν_5 mode is a measure

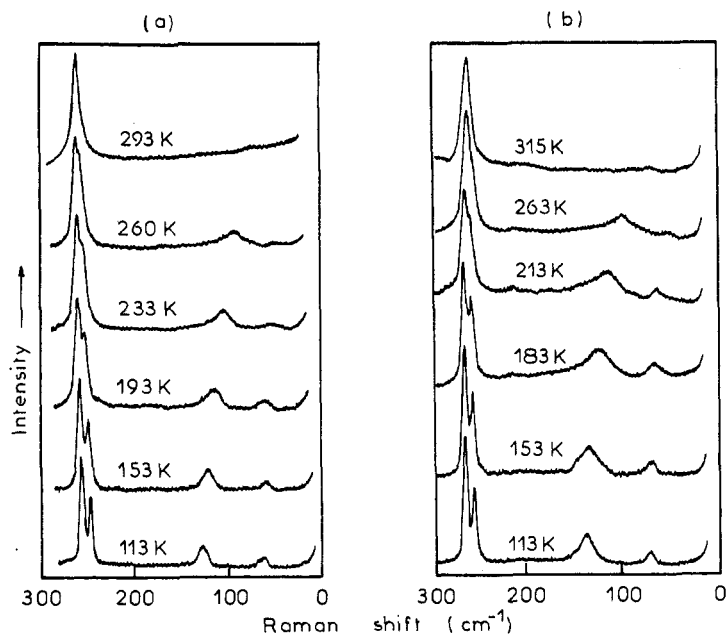


Figure 2. Temperature dependence of the Raman spectra of (a) CoZrF_6 and (b) ZnZrF_6 , through the $Fm\bar{3}m \leftrightarrow R\bar{3}$ structural phase transition.

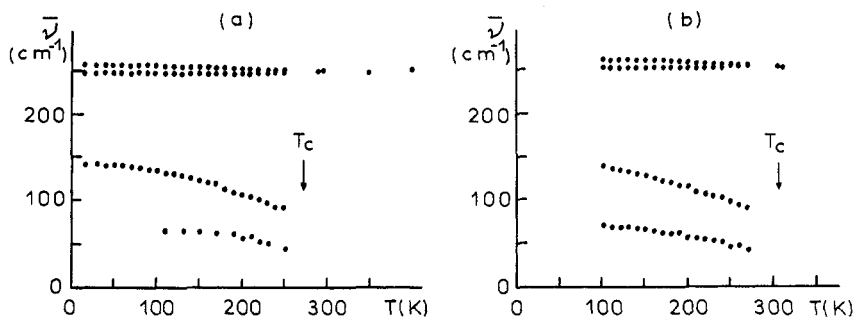


Figure 3. Temperature dependence of the ν_5 and ν_R mode frequencies in (a) CoZrF_6 and (b) ZnZrF_6 , through the $Fm\bar{3}m \leftrightarrow R\bar{3}$ structural phase transition.

of the internal distortion of the octahedra, already evidenced in the structural study (see paper I [1]). In addition, an important softening of both components of ν_R is observed when the transition temperature is approached from below (figure 3). This effect clearly proves the existence of a displacive contribution in the transition mechanism, arising from octahedra rotations. The behaviour of these soft modes can be fully understood in the framework of Landau theory (see paper III). It should also be pointed out that both components of ν_R become heavily damped in the high-temperature range of $R\bar{3}$ phase (figure 2) and give rise, just below T_c , to a featureless background where the ν_R characteristic frequencies can no longer be determined. This phenomenon might be

related to precursor effects of octahedra orientational disorder, which has been established in the cubic phase by means of x-ray diffuse scattering experiments [1]. Thus, this is possibly a case of intermediate behaviour between true displacive and order-disorder regimes.

5. Conclusions

The experimental data obtained by combined studies of $M^{II}ZrF_6$ ordered fluorides ($M^{II} = Co, Zn$) by means of Brillouin and Raman scattering measurements show that the $Fm\bar{3}m \leftrightarrow R\bar{3}$ structural phase transition occurring in these materials is 'improper' ferroelastic, driven by optical soft modes due to $M^{II}(Zr)F_6$ octahedra rotations (displacive mechanism). An intermediate behaviour between true displacive and order-disorder regimes probably takes place in the vicinity of the transition temperature.

References

- [1] Rodriguez V, Couzi M, Tressaud A, Grannec J, Chaminade J P and Soubeyroux J L 1990 *J. Phys.: Condens. Matter* **2** 7373–86
- [2] Rodriguez V and Couzi M 1990 *J. Phys.: Condens. Matter* **2** 7395–406
- [3] Cowley R A 1980 *Adv. Phys.* **29** 1
- [4] Cavagnat R, Cornut J C, Couzi M, Daleau G and Huong P V 1978 *Appl. Spectrosc.* **32** 500
- [5] Ecolivet C, Sanquer M, Pellegrin J and Dewitte J 1983 *J. Chem. Phys.* **78** 6317
- [6] Turrell G 1972 *Infrared and Raman Spectra of Crystals* (London: Academic)
- [7] Poulet H and Mathieu J P 1970 *Spectres de Vibration et Symétrie des cristaux* (Paris: Gordon and Breach) pp 244–5
- [8] Stokes H T and Hatch D M 1988 *Isotropy Subgroups of the 230 Crystallographic Space Groups* (Singapore: World Scientific) p 1-371
- [9] Holakovskiy J 1973 *Phys. Status Solidi b* **56** 615
- [10] Toledano J C 1979 *Phys. Rev. B* **20** 1147
- [11] Toledano J C and Toledano P 1987 *The Landau Theory of Phase Transitions* (Singapore: World Scientific) pp 193–202
- [12] Rehwald W 1973 *Adv. Phys.* **22** 721
- [13] Vacher R and Boyer L 1972 *Phys. Rev. B* **6** 639
- [14] Born M and Huang K 1954 *Dynamical Theory of Crystal Lattices* (Oxford: Clarendon) pp 373–81
- [15] De Beer W H J, Heyns A M, Richter P W and Clark J B 1980 *J. Solid State Chem.* **33** 283
- [16] De V Steyn M M, Heyns A M and English R B 1984 *J. Crystallogr. Spectrosc. Res.* **14** 505
- [17] Daniel P 1990 *Thesis* University of Maine, Le Mans